Article

Mn(II)-based MRI contrast agent candidate for vascular imaging

Ferenc K. Kalman, Viktoria Nagy, Balázs Váradi, Zoltán Garda, Enik# Molnár,
György Trencsényi, János Kiss, Sandra Même, William Meme, Eva Toth, and Gyula Tircso

Just Accepted

Mn(II)-based MRI contrast agent candidate for vascular imaging

Ferenc K. Kálmán,[1,2] Viktória Nagy,[1] Balázs Váradi,[1] Zoltán Garda,[1] Enikő Molnár,[1] György Trencsényi,[3] János Kiss,[3] Sandra Même,[4] William Même,[4] Éva Tóth*,[4] and Gyula Tircsó*,[1]

[1] Department of Physical Chemistry, H-4032, Debrecen, Egyetem tér 1, Faculty of Science and Technology, University of Debrecen, Hungary

[2] Le Studium, Loire Valley Institute for Advanced Studies, 1 Rue Dupanloup, 45000 Orléans, France

[3] Division of Nuclear Medicine, Department of Medical Imaging, Faculty of Medicine, University of Debrecen, H-4032 Debrecen (Hungary)

[4] Centre de Biophysique Moléculaire, CNRS-UPR 4301, Université d'Orléans, Rue Charles Sadron, CS 80054, 45071 Orléans, France

Supporting Information Placeholder

ABSTRACT: Toxicity concerns related to Gd(III)-based MRI agents prompted an intensive research towards their replacement by complexes of essential Mn(II) ion. Here, we report a macrocyclic chelate, [Mn(PC2A-BP)], which possesses high thermodynamic stability and kinetic inertness as well as remarkable relaxivity (r_{1p} = 23.5 mM^{-1}s^{-1}, 20 MHz, 37 °C) in the presence of human serum albumin allowing a significant MRI signal intensity increase in the vasculature even at low dose (25 μmol/kg) of the complex.

INTRODUCTION

Magnetic Resonance Imaging (MRI) has been used in medical diagnosis for its excellent soft tissue imaging capability for decades now. To increase image contrast, MRI relies on contrast agents (CAs).[1] Recently, many specific molecular imaging probes have been proposed to enable visualization of various biomarkers (peptides, enzyme activity, fluctuation in pH, pO_2 concentration of glucose or metal ions such as Ca(II), Zn(II), Cu(II), etc.).[2] Today, commercially available CAs are all Gd(III) complexes (Gd(III)-based CAs = GBCAs) formed with open-chain (linear) or macrocyclic ligands such as DTPA (diethylenetriamine-N,N,N',N'',N''-pentaacetate) and DOTA (1,4,7,10-tetraazacyclododecane-1,4,7,10-tetraacetic acid) or their derivatives. The lustrous history of MRI CAs seems to be undermined by safety concerns reported in the literature since the early 2000s. The emergence of a potentially fatal disease, Nephrogenic Systemic Fibrosis (NSF) in patients with poor renal function triggered by free Gd(III) ions released from CAs[3,4] prompted a still growing interest to find non-Gd(III) alternatives. Later, from 2014, numerous reports have pointed out that multiple GBCA injections may result in Gd(III) accumulation even in patients with healthy kidney function and receiving exclusively macrocyclic GBCAs.[5,6] These concerns have led to definite measures form regulatory agencies in Europe (https://www.ema.europa.eu/en). In 2017, the European Medicines Agency (EMA) suspended marketing authorizations for three out of the total five GBCAs based on a linear ligand and restricted the use of two other agents only for liver imaging complying with important diagnostic need. In parallel, the Food and Drug Administration (FDA) issued a new class of warnings in relation with the use of GBCAs.

For several years, the paramagnetic Mn(II) has been in the forefront of contrast agent research as it is believed to be one of the most promising alternatives to Gd(III).[1] Naturally, when applied in high concentration, Mn(II) also displays toxicity.[7] Mn(II) accumulation in the brain causes a neurological disorder known as manganism, expressing symptoms similar to Parkinson's disease.[8] Therefore, Mn(II)-based agents must also be administered in the form of stable and inert complexes. Unfortunately, the thermodynamic stability and kinetic inertness of Mn(II) complexes are generally lower than that of Gd(III) or other transition metal counterparts, due to the smaller charge and lack of ligand-field stabilization energy (high-spin d^5 electron configuration). Mn(II) complexes formed with open-chain ligands are known to be kinetically labile; few exceptions involve the rigid CDTA and its derivatives (i.e. PyC3A) or PhDTA complexes (structure of the ligands mentioned in the text are included in Figure 1).[9–11] Being an essential metal ion, Mn(II) is efficiently eliminated form the living system, as it was recently demonstrated following injection of the acyclic [Mn(PyC3A)] chelate into rats.[12] On the other hand, for the majority of macrocyclic Mn(II) complexes, either low relaxivity (i.e. non aquated, but inert [Mn(NOTA)]$^-$ or [Mn(DOTA)]$^{2-}$) or limited inertness (bisaquated Mn(II) complexes of 15-membered macrocyclic ligands such as 15Py-aneN$_5$ or 15Py-aneN$_3$O$_2$) seem to limit potential *in vivo* application.[13–15] A compromise between these seemingly contradictory requirements was recently found with Mn(II) complexes of 1,4-DO2A and its amide derivatives (1,4-DO2AM^{Me2}) by M. Botta and coworkers.[16,17] These stable and inert chelates possess an average of 0.9 bound water molecule.

We propose here to consolidate efficient relaxation enhancement and kinetic inertness by using the pyclen platform for Mn(II) complexation. Recent data on trisubstituted cyclododecanes have evidenced greater conditional stability for [Mn(PCTA)]$^-$ than for [Mn(DOTA)]$^{2-}$ (pH=7.4). The kinetic inertness of [Mn(PCTA)]$^-$ was also found sufficiently high to allow for further ligand modification, such as reduction of ligand denticity to attain higher hydration number of the Mn(II) complex. Recently, we have proposed the PC2A-EA ligand as a

pH responsive CA candidate which merges the advantageous Mn(II) binding properties of PCTA and the pH-responsive "on/off" coordination feature of the ethylamine pendant arm.[18] Following a similar strategy, we have replaced one acetate arm in PCTA with a biphenyl "anchor", resulting in the hexadentate PC2A-BP chelator (Chart 1., see ESI for other structures discussed). With this, we aimed to preserve strong and inert metal coordination by the PC2A chelator, implying monohydration in its Mn(II) complex, while introducing a hydrophobic moiety with potential targeting capability to Human Serum Albumin (HSA). Recent advances in MR hardware enable high quality MR angiography to be performed with extracellular CAs just seconds after injection, and therefore the development of new angiographic CAs is generally considered less important.[19] Nevertheless, specific applications, such as highlighting microvascularization in tumors, would largely benefit from efficient angiographic probes, and in general, HSA remains an important target when it comes to targeted imaging applications.[20–23]
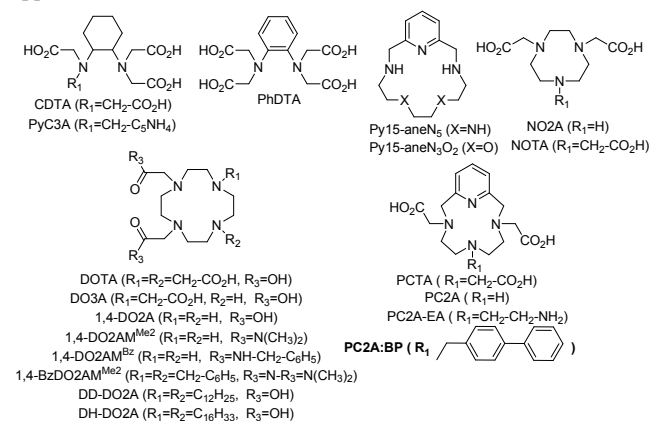

Chart 1. Formulae of the ligands mentioned in the text.

The biphenyl substituent is expected to have an additional positive consequence, important for the safety profile of the complex. The presence of bulky aromatic groups (such as benzyl, methyl-biphenyl etc.) should result in lowering the protonation constant of the ligand in agreement with numerous examples of EDTA- and DTPA-derivatives (Table S1), through steric effect, conformational changes, or by altering the lipophilic/lipophobic balance.[24–26] Moreover, the bulkiness of the substituent should limit the formation of dinuclear intermediates which are important in metal-assisted dissociation pathways, further increasing the kinetic inertness of the Mn(II) chelate.

We show here that the [Mn(PC2A-BP)] complex retains indeed excellent thermodynamic stability and resistance to dissociation. ^{1}H and ^{17}O NMR relaxometric studies evidence monohydration and efficient relaxation enhancement for the complex. [1]H-relaxometry was used to show interaction of [Mn(PC2A-BP)] with HSA. Finally, we demonstrate the capability of the agent to efficiently highlight microvascularization *in vivo* in mice brain.

RESULTS AND DISSCUSSION

PC2A-BP was prepared by alkylating the *bis*-methylcyanide-pyclen precursor, obtained by following the procedure of Kim et al., with commercially available 1-(chloromethyl)-4-phenylbenzene in the presence of DIPEA base and KI.[27] The product was then hydrolyzed in 6 M HCl and purified for analytical work by preparative HPLC to give the PC2A-BP chelator (Scheme 1). In order to get insight into solution equilibria of the PC2A-BP ligand and its complexes formed with

biologically relevant metal ions (Mg(II), Ca(II), Mn(II), Zn(II) and Cu(II)), ligand protonation constants as well as protonation
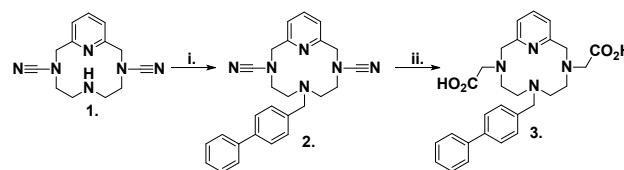
Scheme 1. Synthesis of PC2A-BP ligand: i. 4-phenylbenzyl chloride, DIPEA, KI, MeCN; ii. HCl, than HPLC separation.

and stability constants of the complexes were assessed by pH-potentiometry and supplemented by [1]H-relaxometry (Mn(II)) or UV-vis spectrophotometry (Cu(II)). Protonation constants of the ligand and stability constants of the PC2A-BP complexes are listed in Table 1 along with the corresponding values for PC2A and PCTA (see equations describing the protonation and complex formation equilibria in the experimental part). PC2A-BP is less basic than PC2A which is the consequence of multiple effects (steric, lipophilic/lipophobic equilibrium, changes in conformation or hydrogen binding etc,) associated with the biphenyl unit attached to the nitrogen in *trans* position with respect to the pyridine. PCTA is even less basic, which can be related to the formation of a relatively stable complex with Na^{+}, present at high concentration (ionic strength). Indeed, the protonation constants determined for PCTA in 1.0 M KCl are considerably higher than those determined in the current study in 0.15 M NaCl.[28] The increasing negative charge of the ligands (*i.e.* increasing number of carboxylate groups capable of binding Na^{+} ions) is expected to enhance the stability of the Na^{+} complex, as it was also evidenced for cyclen-based chelators which follow the stability order 1,4-DO2A<DO3A<DOTA.[13,16]

Table 1. Protonation constants of the PC2A, PC2A-BP, and PCTA ligands as well as protonation and stability constants of their complexes (25 °C, I=0.15 M NaCl).

	PC2A-BP	PC2A[b]	PCTA[e]
$\log K_1$	10.45(2)	12.25	9.97; 11.36[f]
$\log K_2$	6.93(3)	5.97	6.73; 7.35[f]
$\log K_3$	2.36(4)	3.47	3.22; 3.83[f]
$\log K_4$	1.64(4)	1.99	1.40; 2.12[f]
$\sum \log \beta_2^H$	17.38	18.22	16.70; 18.71[f]
$\log K_{MgL}$	6.51(6)	9.78	12.35[f]
$\log K_{MgL}^H$	–	–	3.82[f]
$\log K_{CaL}$	7.94(2)	9.90	12.72[f]
$\log K_{CaL}^H$	–	–	3.79[f]
$\log K_{MnL}$	14.86(1)	17.09	16.83
$\log K_{MnL}^H$	–	2.14	1.96
$\log K_{ZnL}$	18.05(1)	19.49[c]	20.48[f]
$\log K_{ZnL}^H$	1.71(2)	2.74[c]	3.10[f]
$\log K_{CuL}$	22.3(2)[d]	23.58[c]	18.79[f]
$\log K_{CuL}^H$	1.04(3)[d]	2.12[c]	3.58[f]
pMn[a]	8.35	8.64	9.74

[a] pMn=-log[Mn(II)], $c_{Mn(II)}=c_{lig}$=0.01 mM ; [b] V. Nagy, K. Póta, E. Tóth, Z. Garda, J. L. Barriada, R. Tripier, C. Platas-

Iglesias, É. Tóth, Gy. Tircsó, manuscript in preparation, 25 °C, I=0.15 M NaCl; [c] determined by simultaneous fitting of pH-pot. and UV-Vis spectrophotometric data; [d] determined by UV-Vis spectrophotometry, [e] 25 °C, I=0.15 M NaCl; [f] Ref [28], 25 °C, I=1.0 M KCl log K_5=1.29.

The stability constants of the complexes increase with increasing basicity of the ligand except for the Cu(II) ion, for which the observed anomaly can be explained in terms of a likely underestimated stability constant for the Cu(PCTA) complex. As it was shown recently for several Cu(II) complexes formed with macrocyclic ligands, pH- potentiometric titrations solely (as it was done for the Cu(PCTA) complex previously) may return erroneous stability constants.[29,30]

PCTA forms a very stable Mn(II) complex and the removal of one metal binding function does not reduce stability (log K_{MnL}=16.83 and 17.09, for PCTA and PC2A, respectively). However, a noticeable decrease is observed upon the attachment of the electron-withdrawing biphenyl entity to PC2A (log K_{MnL}=14.86). The equilibrium model used for the analysis of the pH-potentiometric data has been confirmed with pH depend ent ^{1}H relaxometry (Fig. S1), which also evidenced complete formation of the [Mn(PC2A-BP)] complex by pH=4.5. For the Cu(II) system, complex formation is quantitative already at pH=1.6, thus UV-Vis spectrophotometric titration in batch samples (Fig. S2) was used (22 samples in the [H$^+$] concentration range of 0.003-1.030 M, Fig. S2) to obtain the stability constant.

Stability constants alone do not allow comparing the capability of ligands with different basicity to sequester a given metal cation, as metal complexation and ligand protonation are competitive processes. pM values, defined as -log [M^{m+}]$_{free}$, give a more realistic picture about the conditional stability of the complexes at a given pH. The pMn values calculated at pH=7.4 and c_{Mn}=c_L=0.01 mM[14] for [Mn(PC2A)] and [Mn(PC2A-BP)] are almost identical, while it is one order of magnitude higher for [Mn(PCTA)]$^-$. Under these conditions, for [Mn(PC2A-BP)] less than 0.1% of total Mn(II) is non-chelated in equilibrium making it one of the most stable monoaquated Mn(II) complexes reported to date. Indeed, its pM value is very close to that of the highly stable, but non-hydrated [Mn(DOTA)]$^{2-}$ complex (pMn=9.02).[13]

The thermodynamic stability of the Zn(II) and Cu(II) complexes is orders of magnitude higher than that of the Mn(II) analogues (Table 1), in agreement with the Irving-Williams series. For this reason, the inertness of the Mn(II) complexes designed for MRI applications has to be particularly high to minimize Mn(II) release that could result from exchange reactions with endogenous ligands and metal ions. The inertness of [Mn(PC2A-BP)] was assessed by monitoring metal exchange reactions in the presence of high (10−40 fold) excess of Cu(II) ion, in the pH-range 3.3-5.0. Typically, Mn(II) and Gd(III) complexes follow analogous dissociation pathways (Scheme S1). These involve (i) spontaneous dissociation, (ii) proton-assisted pathways through the formation of protonated complexes or (iii) metal-assisted dissociation, occurring *via* direct attack of the exchanging metal ion on the protonated or deprotonated complex and the subsequent formation of a dinuclear intermediate (see SI for detailed description). Under pseudo-first-order conditions as applied in our study, the rate of the decomplexation can be drawn as in eqn. 1:

$$-\frac{d[Mn(PC2A\text{-}BP)]_t}{dt} = k_{obs}[Mn(PC2A\text{-}BP)]_t \qquad \text{Eqn. 1.}$$

where k_{obs} is a pseudo-first-order rate constant and [Mn(PC2A-BP)]$_t$ is the total concentration of the Mn(II) chelate.

The k_{obs} values increase with increasing H$^+$ concentration, while remain independent of Cu(II) concentration, indicating the absence of a metal-assisted pathway (Figure 1). Taking into account the concentration of the protonated and deprotonated complexes ([Mn(PC2A-BP)]$_t$=[Mn(PC2A-BP)]+[Mn(HPC2A-BP)]) as well as the protonation constant of [Mn(PC2A-BP)] (K_H), the following rate equation can be derived (eqn. 2):

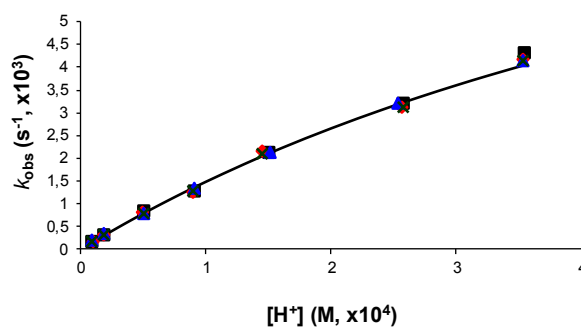$$k_{obs} = \frac{k_0 + k_1[H^+]}{1 + K_H[H^+]} \qquad \text{Eqn. 2.}$$

Figure 1. Dependence of the pseudo-first-order rate constants (k_{obs}) on the concentration of H$^+$ and Cu(II) ions for the [Mn(PC2A-BP)] complex. The excess of the exchanging metal ion was ×10(■),×20(♦), ×30(▲) and ×40(×) folds. The line corresponds to the best fit of the k_{obs} values to eqn. 2.

The fit of the k_{obs} values to equation 2 revealed that spontaneous dissociation is negligible (k_0 is zero). Thus the dissociation of the complex occurs exclusively through the proton-assisted pathway, with a rate constant of k_1 = 16.9±0.2 M^{-1}s^{-1}. The protonation constant of [Mn(PC2A-BP)] obtained is K_H=1350±110 M^{-1}, one order of magnitude lower than that for [Mn(PC2A)], reflecting the lower basicity of PC2A-BP. Nevertheless, the proton-assisted dissociation of [Mn(PC2A-BP)] is over 200 times faster than that of [Mn(PCTA)]$^-$ ($k_1^{[Mn(PCTA)]}$=0.082 M^{-1}s^{-1}).[13] In contrast to [Mn(PC2A)] and [Mn(PCTA)]$^.$ the metal-assisted pathway is not active for [Mn(PC2A-BP)]. It is the consequence of the steric hindrance induced by the biphenyl moiety inhibiting any structural reorganization of the [Mn(PC2A-BP)] chelate that would be necessary to form a dinuclear intermediate. The lack of such metal-assisted pathway is responsible for the remarkable inertness of [Mn(PC2A-BP)]. At pH=7.4 and 25 °C, the dissociation half-life is $t_{1/2}$=286.2 hours for [Mn(PC2A-BP)], one order of magnitude higher than $t_{1/2}$=21.0 h for [Mn(PC2A)], though lower than $t_{1/2}$=5.9×10^4 h for [Mn(PCTA)]. The $t_{1/2}$ value calculated for [Mn(PC2A-BP)] is the half of that found for the [Mn(1,4-DO2AM^{Me2})]$^{2+}$ complex, while the Mn(II) complex formed with a structurally related PC2A-EA ligand appears to be notably more inert ($t_{1/2}$=8×10^3 h).[17,18] Considering a 3-4–fold acceleration of the dissociation with the increase of temperature on going from 25 °C to 37 °C, one can estimate a half-life ($t_{1/2}$) of 72-95 hours for [Mn(PC2A-BP)] at physiological temperature which implies that substantial amount of the complex injected expected to be excreted intact (see SI for details) and the Mn(II) released *in vivo* from the complex is estimated to be below 1 mg (when applied at 0.3 mmol/kg in a 70 kg patient). Expectedly, the body can handle

such low amounts of free Mn(II) without consequences on safety. These considerations are also in full accordance with the results of P. Caravan and co-workers who observed indeed very efficient elimination of the Mn(II) after injection of $[Mn(PyC3A)]^-$ in rats.[12] Finally the stability test performed with the use of Seronorm solution have also confirmed the exceptional inertness of the complex (Fig S3).

The water-exchange rate, an important parameter that contributes to efficient relaxation enhancement, was determined by measuring the ^{17}O transverse relaxation rates $(1/T_{2r})$ for an aqueous [Mn(PC2A-BP)] solution and a diamagnetic reference at different temperatures (9.4 T, Figure 2). The ^{17}O $1/T_{2r}$ data were analyzed by the Swift-Connick equations[31] assuming a simple exponential behavior of the electron spin relaxation (see SI for details). The hydration number was fixed to $q = 1$ (based on the proton relaxivity and the maximum ^{17}O $1/T_{2r}$ value allowing for an estimation of $q = 0.9\pm0.2$ according to Gale et al. Fig. S4).[32] The activation energy for the electron spin relaxation and the scalar coupling constant were set to E = 1 kJ/mol and $A_O/\hbar = 40\times10^6$ rad s^{-1}, respectively following literature recommendations.[33] The water exchange rate, $k_{ex}^{298}=(6.3\pm0.2)\times10^7$ s^{-1}, its activation enthalpy, $\Delta H^{\neq}=35.7\pm0.1$ kJ/mol, and the electron spin relaxation rate, $1/T_{1e}^{298}=(4.8\pm0.4)\times10^7$ s^{-1} were calculated. The contribution of the electron spin relaxation term to the correlation time $1/\tau_c = k_{ex} + 1/T_{1e}$ is limited at high temperatures (~8 % at 348 K) which allows for an accurate determination of the water exchange rate. The k_{ex}^{298} value obtained for [Mn(PC2A-BP)] is slightly higher than value corresponding to the water exchange rate of [Mn(PC2A-EA)] $(k_{ex}^{298}=4.0\times10^7$ $s^{-1})$,[18] it is the half of that found for [Mn(PC2A)] $(k_{ex}^{298}=15.2\times10^7$ $s^{-1})$ and more than 7 times lower than that of $[Mn(EDTA)]^{2-}$ $(k_{ex}^{298}=47.1\times10^7$ $s^{-1})$.[15]
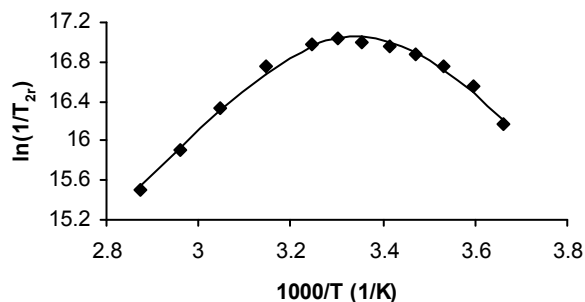

Figure 2. Temperature dependence of the reduced ^{17}O transverse relaxation rates for [Mn(PC2A-BP)] at 9.4 T and pH 7.4. The line corresponds to the best fit of the data.

The difference in the water exchange rate of the [Mn(PC2A-BP)] and [Mn(PC2A)] complexes arises from the presence of the biphenyl pendant which can slow down the rearrangement of the coordination cavity during the water exchange process, similarly to triazacyclononane-diacetates (NO2A) bearing aromatic substituents.[34]

In the presence of 0.7 mM HSA, the relaxivity of [Mn(PC2A-BP)] undergoes a six fold increase (23.5 vs. 3.8 $mM^{-1}s^{-1}$ in the absence of HSA; 37 °C, 0.49 T)[22,23], indicating a strong interaction between the [Mn(PC2A-BP)] complex and the protein (log $K_{aff}=3.4\pm0.1$ and $r_{1p}^b=35.7\pm2.5$ $mM^{-1}s^{-1}$, see ESI for more relaxivity data, Fig S5-S8). The r_{1p}^b value is lower than those observed for the majority of EDTA-like Mn(II) chelates by M. Botta and coworkers, while other EDTA-based HSA targeting

structures showed similar relaxivity and considerably higher (by an order of magnitude) affinity constant (Table S2).[22,35] Similar relaxivity values (r_{1p}^b) and binding constants were observed, however, for Mn(II) chelates formed with DO2A-bis(amide) or amphiphilic DO2A derivative ligands (Table 2).[22,36]

Table 2. Comparison of relaxivities (0.49 T MHz; 298 K) and HSA binding affinities of selected macrocyclic Mn(II) complexes.

	log $(n\times K_{aff})$	r_{1p} $(mM^{-1}s^{-1})$	r_{1p}^b $(mM^{-1}s^{-1})$
[Mn(PC2A-BP)]	3.4±0.1	4.96±0.5	35.7±2.5
$[Mn(BzDO2AM^{Me2}]^{2+,a}$	3.59	3.8	18.5
$[Mn(DO2AM^{Bz}]^{2+,a}$	3.08	3.5	27.4
[Mn(DD-DO2A)] [b]	4.36	12.6	29.5
[Mn(DH-DO2A)] [b]	4.00	15.3	27.2

[a] ref. [36]; [b] ref. [22]

The efficacy of the [Mn(PC2A-BP)] complex as an HSA targeting probe was evaluated in MRI experiments at 3 T magnetic field strength by using phantoms with 0.20 mM complex in seronorm or in the presence of 0.7 mM HSA (Fig S10). Analysis of the MR images indicate that the signal intensity changes notably on going form $[Mn(CDTA)]^{2-}$ to [Mn(PC2A-BP)] alone, but more pronounced brightening of T_1 images is observed when the HSA (or other proteins present in the serum) appears in the sample.

HSA is an important protein target for angiographic imaging and the potential of [Mn(PC2A-BP)] for the visualization of the vascular system has been demonstrated in an angiographic MRI study in Swiss mice.[19,37] MR dynamic contrast enhanced (DCE) imaging has been performed in Swiss mice to follow the biodistribution of [Mn(PC2A-BP)]. After the injection of the complex, there is an immediate increase in signal intensity in the kidney, followed by a decrease. This indicates that a part of the contrast agent is excreted via the kidneys. This elimination phase is quicker than that for the Dotarem, a GBCA used in clinical practice ([Gd(DOTA)]Meg). In parallel, intensity also increases in the liver and remains constant for a period of 15 minutes (Fig. S10). This is likely the cumulative effect of some hepatocellular uptake and the presence of the agent in the blood vessels of the highly vascularized liver. The signal intensity increase in the liver is less pronounced than that in the kidney medulla. Vascular cerebral blood flow was measured by Magnetic Resonance Angiography (MRA) using a Fast Low Angle Shot (FLASH) sequence at an injected dose of 25 µmol/kg of [Mn(PC2A-BP)], which is 4 times smaller than the standard dose of the Gd(III)-based MRI CAs used for clinical experiments. [Mn(PC2A-BP)] provided a substantial increase in blood signal that allowed the visualization of brain vascularization in more details than without
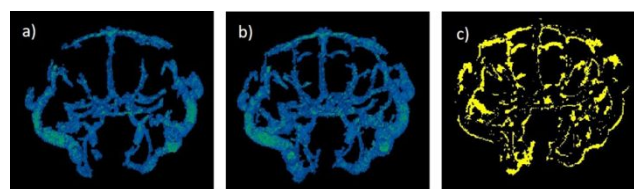

Figure 3. Angiographic MR images of a Swiss mouse brain acquired (a) before and (b) 30 min after i.v. administration of

[Mn(PC2A-BP)] at a dose of 25 µmol/kg, using a FLASH sequence (FOV =1.83*1,83 cm, x 14 mm2, matrix = 256 x 256, TR/TE = 30/5 ms, 51 axial slices 0.2 mm thickness, NA = 4, experimental time = 13 min). (c) Signal intensity increase observed at 30 min post-injection with respect to the pre-injection angiographic MR image.

the CA. It highlighted micro-vascularization which was invisible without injecting the chelate as demonstrated in Figure 3 which represents pre- and post-injection angiographic MR images as well as the signal intensity difference between the two. The increase in blood signal intensity was retained even 30 minutes after the injection, and could be quantified as +26% at this time point with respect to the signal intensity prior to injection. MRA can be typically performed without the use of contrast agents or with extracellular fluid agents like Magnevist ([Gd(DTPA)]Meg$_2$) and Dotarem by imaging few seconds after injection during the first pass of the agent through the vasculature.[19] Nevertheless, a substantial improvement in highlighting the microvessels, otherwise invisible, and the extension of the time window available for imaging can be beneficial in certain cases, such as in characterizing the tumor vascularization.

CONCLUSION

In conclusion, we have demonstrated that the PC2A platform and in particular the PC2A-BP is a promising chelator for Mn(II). The chemical design involving a bulky substituent on the macrocycle nitrogen prevents metal-assisted dissociation pathways and induces remarkable inertness ($t_{1/2}$=286.2 hours at 25 °C). This, combined with an excellent thermodynamic stability (log $K_{[Mn(PC2A-BP)]}$=14.86, pMn=8.35), minimizes potential *in vivo* metal release (based on serum stability studies it is estimated below 0.05 %). The high relaxivity observed in the presence of 0.7 mM HSA (r_{1p} = 23.5 mM^{-1}s^{-1}, 20 MHz, 37 °C) allows to considerably lower the injected dose of the CA (25 µmol/kg) and yet to obtain excellent visualization of the mouse brain vasculature.

EXPERIMENTAL SECTION

General Remarks. Starting commercial reagents/solvents were purchased from Sigma-Aldrich (St. Louis, MO, USA), Tokyo Chemical Industry (Tokyo, Japan) and Fluorochem (Hadfield, Glossop, UK) and were used without further purification unless otherwise stated. Deionized Milli-Q® water was used for the preparation of all aqueous solutions (equilibrium/kinetic/relaxometric studies). ^{1}H NMR spectra were recorded on a Bruker Avance 360 or 400 MHz spectrometer (chemical shifts are given as δ values with reference to tetramethylsilane and coupling constants are reported in Hz). Mass spectroscopic characterization of the product was performed in the Laboratory of Instrumental Analysis, Department of Organic Chemistry of the University of Debrecen equipped with Thermo Accela 600 UPLC system coupled with LTQ-XL mass spectrometer. Prior to its use in the analytical experiments, the final product was purified by preparative high-pressure liquid chromatography (HPLC). Analytical HPLC was performed with the a Waters Alliance 2690 HPLC (Waters Inc., USA) system equipped with a Luna C18(2) 150 mm × 4.6 mm, 100Å, 5µm column (Phenomenex Inc., USA), at 25 °C temperature, with a flow rate of 1.00 mL/min. Preparative separations were performed using HPLC technique (YL9100 HPLC, Korea) equipped with a Luna C18(2) column (250 mm × 21.2 mm, 100Å, 5µm, Phenomenex Inc. USA). The solvent flow rate in this case was 25.00 mL/min using gradient elution as follows: eluent A (5 mM TFA in water) and B (ACN); gradient: 15% B to 40% B in

7.50 min. The purity of the product was >99.8 % determined by reverse-phase HPLC with UV-vis detection at 210 and 260 nm (Fig. S12).

Synthesis of the PC2A-BP ligand. The PC2A-BP ligand was prepared by alkylating the bis-methylcianide-pyclen precursor (3,9-bis(methylenenitrile)-3,6,9,15-tetraazabicyclo[9.3.l]-pentadecal(lS),ll,l3-triene 1) prepared by following the procedure of Kim et al.[27] with the commercially available 4-phenylbenzyl chloride in the presence of Hüning's base as follows: 150 mg (0,528 mmol) of bis-methylcianide-pyclen (1) was dissolved in 5 mL of dry acetonitrile under Ar protected atmosphere and 0.185 ml (1.06 mmol) of Hüning's base (*N,N*-diisopropylethylamine, DIPEA) as well as 45 mg (0,268 mmol) of KI was added to the solution. The reaction mixture was heated to 60 °C by using an oil bath and 0.118 g (0.580 mmol) of 4-phenylbenzyl chloride dissolved in 5 mL of dry acetonitrile was added to the suspension dropwise during 3 hours. The reaction mixture was stirred at the given temperature for 40 hours, filtered and the filtrate evaporated to dryness under reduced pressure. The oily residue was redissolved in 10 mL of 12 M HCl and the solution was refluxed for 25 h at 110 °C. The reaction mixture was then evaporated to dryness under reduced pressure and the residue was redissolved in 4 mL of double distilled water. Separation via preparative HPLC (Fig. S12) yielded PC2A-BP as off white solid upon freeze-drying the combined fractions containing the product. Yield 144 mg (81%).

^{1}H-NMR (Fig. S13): (360,13 MHz, D$_2$O) δ = 3.16 (m 4H, >N-**CH$_2$**-CH$_2$-) 3.38 (m 4H, >N-CH$_2$-**CH$_2$-**) 3.74 (s 4H, >N-**CH$_2$**-COOH) 4.26 (s 2H, >N-**CH$_2$**-C$_{12}$H$_9$) 4.52 (s 4H, >N-**CH$_2$**-Py) 7.44 (t 1H, -CH-**CH**-CH- (C$_{12}$H$_9$)) 7.53 (m 2H, -**CH**-CH-**CH**- (C$_{12}$H$_9$)) 7.62 (d 4H, -**CH-CH**- (C$_{12}$H$_9$)) 7.72 (m 2H, -**CH**-CH-**CH**- (Py)) 7.73 (m 2H, -**CH**-C-**CH**- (C$_{12}$H$_9$)) 8.19 (t 1H, -CH-**CH**-CH- (Py)).

^{13}C-NMR (Fig. S13): (100 MHz, D$_2$O) δ = 51.6 (4C, 2p >N-**CH$_2$**-CH$_2$-) 56.6 (4C, 2p >N-**CH$_2$**-COOH and 2p >N-**CH$_2$**-Py) 58.1 (1C, >N-**CH$_2$**-C$_{12}$H$_9$) 123.8 (2C, -**CH**-CH-**CH**- (Py)) 127.1 (1C, -CH-**CH**-CH- (C$_{12}$H$_9$)) 127.8 (4C, 2p -**CH**-C-**CH**- (C$_{12}$H$_9$)) 128.3 (1C, -CH-**CH**-CH- (Py)) 129.3 (2C, -**CH**-CH-**CH**- (C$_{12}$H$_9$)) 131.8 (2C, -**CH**-C(CH$_2$)-**CH**- (C$_{12}$H$_9$)) 139.7 (1C, -CH-**C**(CH$_2$)-CH- (C$_{12}$H$_9$)) 143.6 (2C, 2p -CH-**C**-CH- (C$_{12}$H$_9$)) 151.5 (2C, 2p -CH$_2$-**C**-N$_{py}$) 163.1 (2C, 2p –**C**OOH).

MS (ESI) m/z 489,25(M+H)$^+$ 100%; 542,17(M+Na)$^+$ 15%.

Thermodynamic studies. The highest analytical grade chemicals were used for the studies. The concentration of the metal chloride stock solutions were determined by complexometric titration with the use of standardized Na$_2$H$_2$EDTA and xylenol orange (ZnCl$_2$), murexid (CuCl$_2$), Patton & Reeder (CaCl$_2$) and Eriochrome Black T (MgCl$_2$ and MnCl$_2$) as indicator. Equilibrium studies were performed by pH-potentiometry, with complementary methods applied for Cu(II) (UV-vis) and Mn(II) ([1]H-relaxometry) complexes. Methrohm 888 Titrando titration workstation with a Metrohm-6.0233.100 combined electrode were used to perform the pH-potentiometric titrations. The titrated solutions (6.00 mL) were stirred and thermostated (25 °C) in inert gas (N$_2$) atmosphere to avoid the effect of CO$_2$. For the calibration of the combined electrode, KH-phthalate (pH=4.005) and borax (pH=9.177) buffers were used. The pH-potentiometric titrations were carried out at constant ionic strength (0.15 M NaCl). For determining the concentration and protonation constants of the H$_2$PC2A-BP ligand, pH-potentiometric titrations were made by using 0.2 M NaOH in 2 mM ligand solutions. pH-potentiometry was also used to

determine the protonation and stability constants of the metal complexes (except for Cu(II)) where the metal-to-ligand ratio was 1:1. The concentration of the ligand and metal ion was generally 2 mM. For the calculation of the protonation and stability constants 80-120 mL–pH data pairs obtained in the pH range of 1.7-12.0, were used. By fitting the mL–pH data pairs collected in the ligand titrations to Equation 3, the protonation constants of the ligand were calculated.

$$K_i^H = \frac{[H_iL]}{[H_{i-1}L][H^+]} \quad \text{where } i=1\text{-}4 \qquad \text{Eqn. 3}$$

In the solution equilibria of the PC2A-BP complexes formed with Mg(II), Ca(II), Mn(II), Zn(II) and Cu(II) ions the formation of [MnL] and protonated species [MnHL] was assumed (Equations 4 and 5).

$$K_{MnL} = \frac{[MnL]}{[Mn][L]} \quad \text{Eqn. 4 and} \quad K_{MnL}^H = \frac{[MnHL]}{[MnL][H^+]} \qquad \text{Eqn. 5}$$

For the calculation of H^+ concentrations from the measured pH values a 0.01 M HCl (0.15 M NaCl) solution was titrated with standardized NaOH based on the method proposed by Irving et al..[38] The value of K_w (ion product of water) was obtained from the same titration (pH=11.5-12.0). PSEQUAD program was used to perform the equilibrium calculations. [39]

Because of the high stability of Cu(II) complex formed with PC2A-BP, the complexation is complete even at pH=1.7 which is the lower pH-limit of pH-potentiometric titrations. For this reason, 22 batch samples containing a slight excess (1%) of ligand were prepared (c_{lig}=0.202 mM, $c_{Cu(II)}$=0.200 mM, I=1.0 M (NaCl+HCl), 25 °C). The $[H^+]$ in these samples were varied in the range of 2.936–1027 mM (Fig. S2). The samples were set aside to attain the equilibrium (one day) and the absorption spectra were recorded in the range of 220-400 nm using quarts cuvettes (1.000 cm optical path length) via JASCO V750 UV-Vis spectrophotometer. For the best fit of the spectrophotometric data the molar absorptivity of the species were also fitted.

Kinetic studies. Kinetic studies were performed either by following metal exchange reactions with Cu(II) (UV-vis spectrophotometry) or changes in T_2 relaxation times in the presence of large Zn(II) excess as a function of time as proposed by P. Caravan et. al (at pH=6.0 set by 2-(N-morpholino)ethanesulfonic acid (MES) buffer, using 25 fold excess of Zn(II)).[11] The rates of metal exchange reactions were determined in the pH range 3.4-5.3 by using Cu(II) ion as a ligand scavenger. To ensure the pseudo-first order conditions 10–40-fold excess of the metal ion was used (c[Mn(PC2A-BP)]=0.1 mM). The pH was set by using non-coordinating buffer such as N,N'-dimethyl-piperazine (DMP, log K_2^H=4.18) at 50 mM concentration. For the calculation of the pseudo-first-order rate constants (k_{obs}), the absorbance values measured at different t times were fitted to the following equation:

$$X_t = (X_0 - X_e)e^{-k_{obs}t} + X_e \qquad \text{Eqn. 6}$$

where X_0, X_t and X_e are the absorbance/relaxivity values measured at the start (0), at time t and at equilibrium (e), respectively.

^{1}H-relaxometric studies. Measurements of longitudinal (T_1) and transversal (T_2) relaxation times were performed by using a Bruker Minispec MQ-20 and MQ-60 NMR analyzers working at 0.49 T and 1.41 T (corresponding to 20 MHz and 60 MHz proton Larmor frequency, respectively). The temperature of the sample holder was set (25.0±0.2°C or 37.0±0.2°C) and controlled with the use of a circulating water bath. The T_1 values were determined with the inversion recovery method (180°–τ–90°) by averaging 4-6 data points obtained at 10 different τ delay values. The transverse relaxation times (T_2) were measured by using the Carr-Purcell-Meiboom-Gill sequence (CPMG) sequence by averaging again 4-6 identical data points. The r_{1p} and r_{2p} relaxivities of the complex were determined by using batch samples (in the concentration range of 0.05-1.05 mM) prepared under nitrogen atmosphere having the ligand present at slight excess. The pH in these samples was kept constant at pH = 7.30 with the use of 20 mM HEPES buffer (I=0.15 M NaCl, 25 °C).

Determination of the affinity constant for the [Mn(PC2A-BP)]–HSA system. The binding constants of the [Mn(PC2A-BP)] with HSA was determined following published literature.[40] The nonlinear increase of the proton paramagnetic relaxation rates measured at 0.49 T in solutions containing 0.204 mM complex was titrated with HSA. The diamagnetic relaxivity of the water protons and HSA in aqueous solution was taken into account during the calculation.

^{17}O NMR data acquisition. To assess the water exchange rate of the Mn(II) complex, ^{17}O-NMR studies were performed on a Bruker Avance 400 MHz (9.4 T, 54.2 MHz) spectrometer. T_1 and T_2 relaxation times and chemical shifts of an aqueous solution of the Mn(II) complex (pH=8,0 0.45 mM) and of a diamagnetic reference (HClO$_4$ acidified water, pH = 3.3) were measured in the temperature range 273–348 K. In order to avoid the oxidation of the Mn(II) ion in the complex solution hydroxyl-amine was added to the sample (10 mM concentration). The temperature was determined according to previous calibration routines by means of ethylene glycol as standard. T_1 and T_2 relaxation times were determined by the inversion-recovery and the CPMG spin-echo technique, respectively The technique of the ^{17}O NMR measurements has been described previously.[41,42] To avoid susceptibility corrections of the chemical shifts, a glass sphere fitted into a 10 mm NMR tube was used during the measurements. The sensitivity of ^{17}O-NMR measurements ^{17}O enriched water (10 % H$_2$^{17}O, CortecNet) was added to the solutions to reach a 2 % enrichment. The fit of the ^{17}O NMR data was performed using Micromath Scientist calculation program via least squares fitting procedure.

MR dynamic contrast enhanced imaging (DCE) for contrast agent biodistribution. Animal experiments were performed at Centre de Biophysique Moléculaire (CBM CNRS UPR431) in Orléans, France in accordance to national and European laws and regulations. The project received approval from the "Ministère de l'enseignement supérieur de la recherche et de l'innovation" under the authorization number 20366. We conform to the Council Directive of 24 November 1986 on The Approximation Of Laws, Regulations And Administrative Provisions Of The Member States Regarding The Protection Of Animals Used For Experimental And Other Scientific Purposes (86/609/Eec and 2010/63/EU).

Eight week old female Swiss mice (RjOrl:SWISS, Janvier Labs) were used for the study. During the MR experiments, the mice were positioned in a custom-built cradle to immobilize the body. They were anesthetized during the MR experiment with 1.5% isoflurane and a mixture of O$_2$/air (1:1) with an output of 0.5 l/min. Respiration was monitored during the whole experiment using an air pillow and body temperature was maintained constant at 37 °C by a warm-water circulation system. MR acquisitions were performed on a 7 T horizontal ultra shielded superconducting magnet dedicated to small animal imaging (70/16 Bruker Pharmascan, Wissembourg, France) and equipped

with a 230 mT/m gradient set. A Bruker 38 mm inner diameter bircage coil was used for both 1H transmission and reception. The [Mn(PC2A-BP)] (150 μl, 2 mM, pH=7.4) was injected through a catheter placed in the tail vein. The DCE experiment consisted of a T_1-weighted IR TrueFisp Bruker sequence (FOV = 3*3 cm, matrix =128*96, T_R/T_E = 3/1.5ms, slice thickness=1mm). One sagittal T_1-weighted image was acquired every 5 seconds during 15min. The contrast agent was manually injected 1 min after the beginning of the acquisition. Grey level means in the kidney cortex and medulla were plotted as a function of time during 15 minutes.

Magnetic Resonance Angiography (MRA). Measurements of vascular cerebral blood flow were performed by MRA using a Fast Low Angle Shot (FLASH) sequence, with the following parameters: FOV =1.83*1,83 cm, x 14 mm², matrix = 256 x 256, T_R/T_E = 30/5 ms, 51 axial slices 0.2 mm thickness, NA = 4, experimental time = 13 min. Angiograms were produced by generating maximum intensity projection (MIP) images after interpolating raw data to obtain an isotropic resolution (109 μm³). This sequence was performed before, 15 min and 30 min after contrast agent injection.

AUTHOR INFROMATION

Corresponding Authors

E-mail: eva.jakabtoth@cnrs.fr (E.T.) and gyula.tircso@science.unideb.hu (Gy.T.)

Notes
The authors declare no competing financial interests.

ASSOCIATED CONTENT

Supporting Information

Additional experimental details (including ¹H- and ¹³C-NMR spectra, HPLC trace etc. for PC2A-BP ligand); a scheme illustrating the dissociation mechanism of a Mn(II) chelate; determination of relaxivity at 0.49 and 7 T, pH-profile of the relaxivity; determination of the binding constant for the HSA adduct and binding constants of other Mn(II) chelates; determination of the number of bound water molecules in [Mn(PC2A-BP)] chelate; NMRD profiles obtained in the absence and presence of HSA; equations used during the fitting of ¹H- and ¹⁷O-relaxometric data and additional results of phantom and in vivo (DCE) MRI studies. This material is available free of charge via the Internet at http://pubs.acs.org.

ACKNOWLEDGMENT

ABBREVIATIONS USED

DTPA, diethylenetriamine-N,N,N',N'',N''-pentaacetate; DOTA, 1,4,7,10-tetraazacyclododecane-1,4,7,10-tetraacetic acid; CA, Contrast Agent; GBCA, Gd-Based Contrast Agents; NSF, Nephrogenic Systemic Fibrosis; EMA, European Medicines Agency; CPMG sequence, Carr-Purcell-Meiboom-Gill sequence; $1/T_{2r}$, transverse relaxation rate; DCE imaging, dynamic contrast enhanced imaging; MRA, Magnetic Resonance Angiography; FLASH sequence, Fast Low Angle Shot sequence; FOV, field-of-view; MIP, maximum intensity projection; DIPEA, *N,N*-diisopropylethylamine; MES, 2-(*N*-morpholino)ethanesulfonic acid; DMP, *N,N'*-dimethyl-piperazine, HEPES, 2-[4-(2-hydroxyethyl)piperazin-1-yl]ethanesulfonic acid;

REFERENCES

(1) Doan, B-T.; Meme, S.; Beloeil, J-C. General Principles of MRI. In *The Chemistry of Contrast Agents in Medical Magnetic Resonance Imaging*; Merbach, A., Helm, L., Tóth, É., Eds.; Second edition, John Wiley & Sons Ltd: Chichester, UK, 2013; Vol. 1, pp 1-24.

(2) Parrott, D.; Fernando, W. S.; Martins, A. F. Smart MRI Agents for Detecting Extracellular Events In Vivo: Progress and Challenges. *Inorganics* **2019**, *7*, 18.

(3) Grobner, T. Gadolinium – a Specific Trigger for the Development of Nephrogenic Fibrosing Dermopathy and Nephrogenic Systemic Fibrosis? *Nephrol. Dial. Transpl.* **2006**, *21*, 1104–1108.

(4) Darrah, T. H.; Prutsman-Pfeiffer, J. J.; Poreda, R. J.; Ellen Campbell, M.; Hauschka, P. V.; Hannigan, R. E. Incorporation of Excess Gadolinium into Human Bone from Medical Contrast Agents. *Metallomics* **2009**, *1*, 479.

(5) Kanal, E.; Tweedle, M. F. Residual or Retained Gadolinium: Practical Implications for Radiologists and Our Patients. *Radiology* **2015**, *275*, 630–634.

(6) Kanda, T.; Fukusato, T.; Matsuda, M.; Toyoda, K.; Oba, H.; Kotoku, J.; Haruyama, T.; Kitajima, K.; Furui, S. Gadolinium-Based Contrast Agent Accumulates in the Brain Even in Subjects without Severe Renal Dysfunction: Evaluation of Autopsy Brain Specimens with Inductively Coupled Plasma Mass Spectroscopy. *Radiology* **2015**, *276*, 228–232.

(7) Pan, D.; Schmieder, A. H.; Wickline, S. A.; Lanza, G. M. Manganese-Based MRI Contrast Agents: Past, Present, and Future. *Tetrahedron* **2011**, *67*, 8431–8444.

(8) Cersosimo, M. G.; Koller, W. C. The Diagnosis of Manganese-Induced Parkinsonism. *NeuroToxicology* **2006**, *27*, 340–346.

(9) Pota, K.; Garda, Z.; Kálmán, F. K.; Barriada, J. L.; Esteban-Gómez, D.; Platas-Iglesias, C.; Tóth, I.; Brücher, E.; Tircsó, G. Taking the next Step toward Inert Mn²⁺ Complexes of Open-Chain Ligands: The Case of the Rigid PhDTA Ligand. *New J. Chem.* **2018**, *42*, 8001–8011.

(10) Kálmán, F. K.; Tircsó, G. Kinetic Inertness of the Mn²⁺ Complexes Formed with AAZTA and Some Open-Chain EDTA Derivatives. *Inorg. Chem.* **2012**, *51*, 10065–10067.

(11) Gale, E. M.; Atanasova, I. P.; Blasi, F.; Ay, I.; Caravan, P. A Manganese Alternative to Gadolinium for MRI Contrast. *J. Am. Chem. Soc.* **2015**, *137*, 15548–15557.

(12) Erstad, D. J.; Ramsay, I. A.; Jordan, V. C.; Sojoodi, M.; Fuchs, B. C.; Tanabe, K. K.; Caravan, P.; Gale, E. M. Tumor Contrast Enhancement and Whole-Body Elimination of the Manganese-Based Magnetic Resonance Imaging Contrast Agent Mn-PyC3A. *Invest. Radiol.* **2019**, *54*, 697–703.

(13) Garda, Z.; Molnár, E.; Kálmán, F. K.; Botár, R.; Nagy, V.; Baranyai, Z.; Brücher, E.; Kovács, Z.; Tóth, I.; Tircsó, G. Effect of the Nature of Donor Atoms on the Thermodynamic, Kinetic and Relaxation Properties of

Mn(II) Complexes Formed With Some Trisubstituted 12-Membered Macrocyclic Ligands. *Front. Chem.* **2018**, *6*, 232.

(14) Drahoš, B.; Kotek, J.; Hermann, P.; Lukeš, I.; Tóth, É. Mn^{2+} Complexes with Pyridine-Containing 15-Membered Macrocycles: Thermodynamic, Kinetic, Crystallographic, and ^{1}H/^{17}O Relaxation Studies. *Inorg. Chem.* **2010**, *49*, 3224–3238.

(15) Drahoš, B.; Lukeš, I.; Tóth, É. Manganese(II) Complexes as Potential Contrast Agents for MRI. *Eur. J. Inorg. Chem.* **2012**, 1975–1986.

(16) Garda, Z.; Forgács, A.; Do, Q. N.; Kálmán, F. K.; Timári, S.; Baranyai, Z.; Tei, L.; Tóth, I.; Kovács, Z.; Tircsó, G. Physico-Chemical Properties of Mn^{II} Complexes Formed with *Cis*- and *Trans*-DO2A: Thermodynamic, Electrochemical and Kinetic Studies. *J. Inorg. Biochem.* **2016**, *163*, 206–213.

(17) Forgács, A.; Tei, L.; Baranyai, Z.; Tóth, I.; Zékány, L.; Botta, M. A Bisamide Derivative of [Mn(1,4-DO2A)] - Solution Thermodynamic, Kinetic, and NMR Relaxometric Studies. *Eur. J. Inorg. Chem.* **2016**, 1165–1174.

(18) Botár, R.; Molnár, E.; Trencsényi, G.; Kiss, J.; Kálmán, F. K.; Tircsó, G. Stable and Inert Mn(II)-Based and pH-Responsive Contrast Agents. *J. Am. Chem. Soc.* **2020**. *142*, 1662-1666.

(19) Gale, E. M.; Wey, H.-Y.; Ramsay, I.; Yen, Y.-F.; Sosnovik, D. E.; Caravan, P. A Manganese-Based Alternative to Gadolinium: Contrast-Enhanced MR Angiography, Excretion, Pharmacokinetics, and Metabolism. *Radiology* **2018**, *286*, 865–872.

(20) Wang, J.; Wang, H.; Ramsay, I. A.; Erstad, D. J.; Fuchs, B. C.; Tanabe, K. K.; Caravan, P.; Gale, E. M. Manganese-Based Contrast Agents for Magnetic Resonance Imaging of Liver Tumors: Structure–Activity Relationships and Lead Candidate Evaluation. *J. Med. Chem.* **2018**, *61*, 8811–8824.

(21) Islam, Md. K.; Kim, S.; Kim, H.-K.; Park, S.; Lee, G.-H.; Kang, H. J.; Jung, J.-C.; Park, J.-S.; Kim, T.-J.; Chang, Y. Manganese Complex of Ethylenediaminetetraacetic Acid (EDTA)–Benzothiazole Aniline (BTA) Conjugate as a Potential Liver-Targeting MRI Contrast Agent. *J. Med. Chem.* **2017**, *60*, 2993–3001.

(22) Rolla, G.; De Biasio, V.; Giovenzana, G. B.; Botta, M.; Tei, L. Supramolecular Assemblies Based on Amphiphilic Mn^{2+}-Complexes as High Relaxivity MRI Probes. *Dalton Trans.* **2018**, *47*, 10660–10670.

(23) Troughton, J. S.; Greenfield, M. T.; Greenwood, J. M.; Dumas, S.; Wiethoff, A. J.; Wang, J.; Spiller, M.; McMurry, T. J.; Caravan, P. Synthesis and Evaluation of a High Relaxivity Manganese(II)-Based MRI Contrast Agent. *Inorg. Chem.* **2004**, *43*, 6313–6323.

(24) Miller, J. H.; Powell, J. E. Synthesis and Lanthanide Complex Formation Constants of N'-Benzylethylenediamine-N,N,N'-Triacetic Acid. *Inorg. Chem.* **1978**, *17*, 774–776.

(25) Szabadka, O. Determination of Protonation- and Metal Complex Stability Constants for a Chelating Monomer and Its Immobilized in Polymer Resin. *Talanta* **2003**, *59*, 1081–1088.

(26) Tse, P. K.; Powell, J. E. Study of Structural Influence on the Formation Constants of Lanthanide-Polyamino Polycarboxylate Complexes. *Inorg. Chem.* **1985**, *24*, 2727–2730.

(27) Kim, W. D.; Hrncir, D. C.; Kiefer, G. E.; Sherry, A. D. Synthesis, Crystal Structure, and Potentiometry of Pyridine-Containing Tetraaza Macrocyclic Ligands with Acetate Pendant Arms. *Inorg. Chem.* **1995**, *34*, 2225–2232.

(28) Tircsó, G.; Kovács, Z.; Sherry, A. D. Equilibrium and Formation/Dissociation Kinetics of Some Ln^{III} PCTA Complexes. *Inorg. Chem.* **2006**, *45*, 9269–9280.

(29) Rodríguez-Rodríguez, A.; Garda, Z.; Ruscsák, E.; Esteban-Gómez, D.; de Blas, A.; Rodríguez-Blas, T.; Lima, L. M. P.; Beyler, M.; Tripier, R.; Tircsó, G.; Platas-Iglesias, C. Stable Mn^{2+}, Cu^{2+} and Ln^{3+} Complexes with Cyclen-Based Ligands Functionalized with Picolinate Pendant Arms. *Dalton Trans.* **2015**, *44*, 5017–5031.

(30) Regueiro-Figueroa, M.; Ruscsák, E.; Fra, L.; Tircsó, G.; Tóth, I.; de Blas, A.; Rodríguez-Blas, T.; Platas-Iglesias, C.; Esteban-Gómez, D. Highly Stable Complexes of Divalent Metal Ions (Mg^{2+}, Ca^{2+}, Cu^{2+}, Zn^{2+}, Cd^{2+} and Pb^{2+}) with a Dota-Like Ligand Containing a Picolinate Pendant: Complexes of Dota-Like Ligand Containing a Picolinate Pendant. *Eur. J. Inorg. Chem.* **2014**, 6165–6173.

(31) Swift, T. J.; Connick, R. E. Erratum: NMR-Relaxation Mechanisms of ^{17}O in Aqueous Solutions of Paramagnetic Cations and the Lifetime of Water Molecules in the First Coordination Sphere. *J. Chem. Phys.* **1964**, *41*, 2553–2554.

(32) Gale, E. M.; Zhu, J.; Caravan, P. Direct Measurement of the Mn(II) Hydration State in Metal Complexes and Metalloproteins through ^{17}O NMR Line Widths. *J. Am. Chem. Soc.* **2013**, *135*, 18600–18608.

(33) Esteban-Gómez, D.; Cassino, C.; Botta, M.; Platas-Iglesias, C. ^{17}O and ^{1}H Relaxometric and DFT Study of Hyperfine Coupling Constants in [Mn(H$_2$O)$_6$]$^{2+}$. *RSC Adv.* **2014**, *4*, 7094.

(34) Pujales-Paradela, R.; Carniato, F.; Esteban-Gómez, D.; Botta, M.; Platas-Iglesias, C. Controlling Water Exchange Rates in Potential Mn^{2+}-Based MRI Agents Derived from NO2A^{2-}. *Dalton Trans.* **2019**, *48*, 3962–3972.

(35) Baroni, S.; Colombo Serra, S.; Fringuello Mingo, A.; Lux, G.; Giovenzana, G. B.; Lattuada, L. Synthesis and Relaxometric Characterization of a New Mn(II)-EDTA-Deoxycholic Acid Conjugate Complex as a Potential MRI Blood Pool Agent. *ChemistrySelect* **2016**, *1*, 1607–1612.

(36) Forgács, A.; Tei, L.; Baranyai, Z.; Esteban-Gómez, D.; Platas-Iglesias, C.; Botta, M. Optimising the Relaxivities of Mn^{2+} Complexes by Targeting Human Serum Albumin (HSA). *Dalton Trans.* **2017**, *46*, 8494–8504.

(37) Gale, E. M.; Caravan, P. Gadolinium-Free Contrast Agents for Magnetic Resonance Imaging of the Central Nervous System. *ACS Chem. Neurosci.* **2018**, *9*, 395–397.

(38) Irving, H. M.; Miles, M. G.; Pettit, L. D. A Study of Some Problems in Determining the Stoicheiometric Proton Dissociation Constants of Complexes by Potentiometric Titrations Using a Glass Electrode. *Anal. Chim. Acta* **1967**, *38*, 475–488.

(39) Zékány, L.; Nagypál, I. Psequad. In *Computational Method for Determination of Formation Constants*; Legett, D. J., Eds.; Plenum: New York, 1985; Vol. 1, pp 291–353.

(40) Muller, R. N.; Radüchel, B.; Laurent, S.; Platzek, J.; Piérart, C.; Mareski, P.; Vander Elst, L. Physicochemical Characterization of MS-325, a New Gadolinium Complex, by Multinuclear Relaxometry. *Eur. J. Inorg. Chem.* **1999**, 1949–1955.

(41)　Meiboom, S.; Gill, D. Modified Spin-Echo Method for Measuring Nuclear Relaxation Times. *Rev. Sci. Instrum.* **1958**, *29*, 688–691.

(42)　Micskei, K.; Helm, L.; Brucher, E.; Merbach, A. E. Oxygen-17 NMR Study of Water Exchange on Gadolinium Polyaminopolyacetates $[Gd(DTPA)(H_2O)]^{2-}$ and $[Gd(DOTA)(H_2O)]^-$ Related to NMR Imaging. *Inorg. Chem.* **1993**, *32*, 3844–3850.

1
2
3
4
5
6
7
8
9
10
11
12
13
14
15
16
17
18
19
20
21
22
23
24
25
26
27
28
29
30
31
32
33
34
35
36
37
38
39
40
41
42
43
44
45
46
47
48
49
50
51
52
53
54
55
56
57
58
59
60

1
2
3
4
5
6
7
8
9
10
11
12
13
14
15
16
17
18
19
20
21
22
23
24
25
26
27
28
29
30
31
32
33
34
35
36
37
38
39
40
41
42
43
44
45
46
47
48
49
50
51
52
53
54
55
56
57
58
59
60

SYNOPSIS TOC